12-2022

Study of Dual-Tapered Manifold Microgap Spacing and Taper Angle on Pool Boiling Characteristics

Chad Wake
caw5317@rit.edu

R.I.T

Study of Dual-Tapered Manifold Microgap Spacing and Taper Angle on Pool Boiling Characteristics

By

Chad Wake

A Thesis Submitted in Partial Fulfillment of the Requirements for the

Degree of Master of Science in Mechanical Engineering

Thermal Analysis, Microfluidics and Fuel Cell Lab,

Department of Mechanical Engineering

Kate Gleason College of Engineering

ROCHESTER INSTITUTE OF TECHNOLOGY

Rochester, New York

December 2022

Study of Dual-Taper Manifold Microgap Spacing and Taper angle on Pool Boiling Characteristics

By: Chad Wake

A Thesis Submitted in Partial Fulfilment of the Requirements for the Degree of Master of Science in Mechanical Engineering

Department of Mechanical Engineering

Kate Gleason College of Engineering

Rochester Institute of Technology

Approved by:

Dr. Satish Kandlikar

Thesis Advisor *Date*

Department of Mechanical Engineering

Dr. Michael Schertzer

Thesis Committee Member *Date*

Department of Mechanical Engineering

Dr. Robert Stevens

Thesis Committee Member *Date*

Department of Mechanical Engineering

Dr. Sarilyn Ivancic

Department Representative, Thesis Committee Member *Date*

Department of Mechanical Engineering

Abstract

The miniaturization of electronic components has resulted in higher heat generation on a smaller surface area, creating a desire for better heat removal techniques and systems. To improve the performance of the pool boiling system, high critical heat flux and low surface temperatures are desired for efficient heat removal. External structures are one technique that seeks to improve pool boiling performance by passively regulating the flow of vapor away from the boiling surface. The present work seeks to study the effect of dual-taper manifold inlet gap height and taper angle on boiling performance through a parametric study with a copper boiling surface of 34.5 mm x 32 mm. perfluoromethylcyclopentane (PP1C) was used in a closed loop pool boiling system at atmospheric pressure. The current study looks at the design parameters of the dual-taper manifold to study the effect on boiling performance by testing dual-taper manifolds with 0.5mm, 1mm, and 1.5mm inlet gap heights and 10, 15, and 20 degree taper angles and comparing the results to those obtained from a plain test chip. At 0.5mm, critical heat flux (CHF) was worse overall, while heat transfer coefficient (HTC) only showing marginal improvement with a 20 degree taper angle. At 1mm manifold height, CHF was improved at 15 and 20 degree taper angles, while HTC improved with 10 and 15 degree taper angles. At 1.5mm, CHF was slightly reduced at 10 and 20 degree taper angle while marginally improved with a 15 degree taper angle, while peak HTC was marginally improved for all taper angles. The overall poor performance is attributed to long residence time and the poor liquid-vapor density of PP1C and dual-tapered manifolds are not recommended as a pool boiling enhancement technique with similar fluids.

Acknowledgements

I would like to sincerely express my gratitude to Dr. Satish Kandlikar for giving me this opportunity to work at the Thermal Analysis, Microfluidics and Fuel Cell Laboratory. This work would not be possible without his constant support, guidance, and motivation. I would also like to thank the members of my committee: Dr. Satish Kandlikar, Dr. Michael Schertzer, Dr. Robert Stevens, and Dr. Sarilyn Ivancic for their support in evaluating my thesis.

I would also like to thank the Machine Shop faculty, Jan Maneti, Craig Arnold, and Ricky Wurzer, for their help in modifying the experimental setup.

Furthermore, I would also like to thank Maharshi Shukla and the other TAMFL members for their support, encouragement, and laughs.

Finally, I would like to thank my family for supporting me in my pursuit of a master's degree.

TABLE OF CONTENTS

LIST OF FIGURES

LIST OF TABLES

Nomenclature

q''	heat flux (W/cm^2)
CHF	Critical Heat Flux (W/cm^2)
HTC	Heat Transfer Coefficient (W/m^2-K)
θ_t	Taper angle (degrees)
h_t	Taper gap (mm)
W_{sup}	Wall superheat (°C)
T_1	Temperature recorded by thermocouple 1 (°C)
T_2	Temperature recorded by thermocouple 2 (°C)
T_3	Temperature recorded by thermocouple 3 (°C)
T_4	Temperature recorded by thermocouple 4 (°C)
T_{surf}	Extrapolated test chip surface temperature (°C)
T_{sat}	Refrigerant Saturation Temperature (°C)
Δx	Thermocouple spacing between thermocouples 1 and 2 and thermocouples 2 and 3 (mm)
Δy	Spacing between thermocouple 4 and heater surface (mm)

1. Introduction

Over the last several decades, electronic devices have seen increased performance and smaller component footprints. Previously, the issue of thermal management for these devices was solved with a simple fan that forced air over the component to remove heat or relied entirely on passive air flow. However, increasing the performance of the component tends to increase the heat produced while reducing the size reduces the size will reduce both the heat capacity and accessible heat transfer area for that component, resulting in that component heating up faster and requiring a cooling system for that component to operate at that performance specification for a given length of time. Two-phase cooling is good solution to this dilemma. In the scope of desktop computers: single-phase air or liquid cooling are used to cool the CPU, while two-phase cooling is uncommon and more complex to implement. The flow in two-phase cooling is either actively driven by a pump or passively driven by buoyant or similar forces acting to carry the produced vapor phase away from the surface. The performance of the two-phase system is limited by critical heat flux (CHF), where the boiling surface is blanketed by an insulating vapor layer. The heat transfer coefficient of the system can be interpreted as the how efficiently the system can dissipate thermal energy. A high-performance boiling system would be able to dissipate large amounts of heat while keeping the surface temperature as low as possible. Recent research in the field of two-phase cooling have studied various surface modification methods such as modifying the surface, or placing different manifold structures close to the surface to improve the performance of heat transfer.

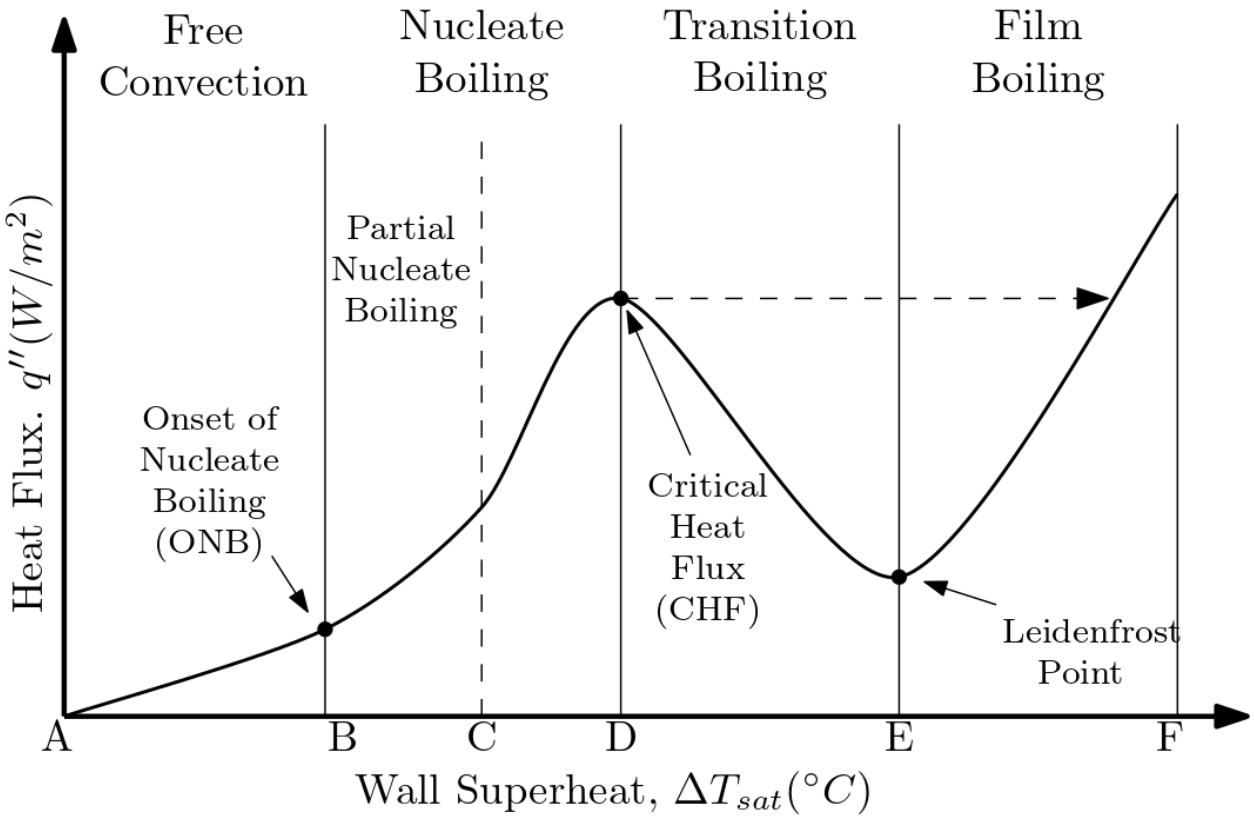

Figure 1. Pool Boiling Curve.

1.1 Pool Boiling Heat Transfer

Pool boiling is well established, where there are no components actively pumping the liquid phase, instead, flow is driven primarily by gravity and buoyant forces acting to remove vapor. The basis of pool boiling is the heater is superheated beyond the boiling point temperature of the working fluid, which transfers heat to the liquid phase, and uses the latent heat of vaporization to remove heat from the surface when the liquid is turned into vapor and is carried away from the surface by buoyant forces.

1.1.1 Free Convection

At low wall superheats, no vapor bubbles are formed. Instead, heat transfer is driven by convection currents near the heater surface. This happens until the heat flux supplied to the heater is raised to the point where the system reaches the onset of nucleate boing.

1.1.2 Nucleate Boiling

Onset of nucleate boiling

The point where nucleate boiling begins is called the onset of nucleate boiling (ONB). This corresponds to the heat flux where vapor bubbles first start to nucleate on the heater surface and is shown at point B on Figure 1.

Nucleate Boiling

The region between B and C in Figure 1 corresponds to the partially developed nucleate boiling region. Here, vapor bubbles nucleate, grow, and depart, before allowing liquid to flow back to the surface before another bubble nucleates. Increasing the heat flux further brings the system to the fully developed nucleate boiling shown between C and D in Figure 1. Here, nucleate boiling has fully developed and bubbles coalesce to form columns of bubbles or continuous jets of vapor on the heater surface.

1.1.3 Critical Heat Flux

Critical heat flux is the point where the boiling surface is functionally saturated with nucleating bubbles, transferring the most heat possible through discrete nucleating bubbles and is shown at point D in Figure 1.

This is a local maximum on the boiling curve and is the upper stability limit of nucleate boiling. At this point, increasing the heat flux supplied to will trip the system directly into the inefficient film boiling mode

1.1.4 Transition Boiling

Transition Boiling is the unstable boiling regime shown between D and E in Figure 1 where vapor films form over parts of the heater surface, while the rest resembles nucleate boiling. The vapor films obstruct the surface, and do not allow liquid to contact the surface at those points, making heat transfer to the liquid phase very inefficient.

1.1.5 Film Boiling

When Critical Heat flux is reached, Bubbles nucleate, grow and coalesce before departing the surface before allowing liquid to rewet to the surface. At CHF, vapor production and heat dissipation is maximized for this bubble formation cycle, Exceeding CHF causes the bubbles to grow and propagate beyond this capacity and occupies most of the heater surface, limiting the ability of the liquid to rewet to the surface. The vapor quickly occupies the whole surface, obstructing any liquid from contacting the surface. To reject the heat and form more vapor, the heat will be transferred from the surface to the liquid primarily by radiation and conduction through the vapor phase, requiring a higher temperature difference to dissipate the heat flux as the thermal resistance is higher than if heat were conducted directly to the liquid phase. The lowest heat flux able to be transferred in this mode corresponds to the leidenfrost point, which is the lower limit of stability for film boiling and decreasing the heat flux at this point will return the system to the nucleate boiling regime.

2. Literature Review

2.1 Pool Boiling With Refrigerants

Rainey and you [1] studied the effect of heater size and orientation on pool boiling heat transfer from micropourous surfaces. They studied the heaters of 2x2 cm and 5x5 cm copper surfaces of pool boiling with FC-72 on plain and microporous coated surfaces. They found that performance saw slight improvement as the surface was inclined from 0 to 45 degrees and increasing the heater size diminished the enhancement at lower heat fluxes and improved the enhancement at higher heat fluxes, but saw substantial decreases from 90 to 180 degrees. The main relevant results is that critical heat flux inversely proportional to heater size and the ability to effectively remove vapor from the surface is important for effective heat transfer at higher heat fluxes.

2.2 Tapered Manifolds In Flow Boiling

Mukherjee and Kandlikar [2] numerically studied inlet constriction on bubble growth during flow boiling in microchannels. Numerically simulated a water bubble nucleating in a uniform cross-section channel .They found that introducing a restriction at the inlet caused bubbles to favor growing in the downstream direction that has comparatively less flow resistance, resulting in stable flow boiling. They proposed diverging channel geometry to achieve this growth direction bias instead of restricting the flow upstream in the system.

Kalani and Kandlikar [3] studied the effect of combining liquid inertia with pressure recovery effects from bubble expansion to enhance flow boiling from microchannels with water as the working fluid. They used 6% taper and 200μm channel width, channel depth, and fin widths, with flow rates ranging from 140 to 300 mL/min. Finding that the effects from liquid inertia and bubble growths can combine and keep a low pressure drop across the region and facilitating uniform saturation temperature. However, increasing the flow rate increases performance up to a

maximum, and further increasing flow rate causes liquid inertia to interfere with bubble nucleation, growth, and departure. Solutions preventing overshooting this maximum to this would be actively controlling flow based upon bubble formation, or having the flow be passively dictated by bubble emergence dynamics.

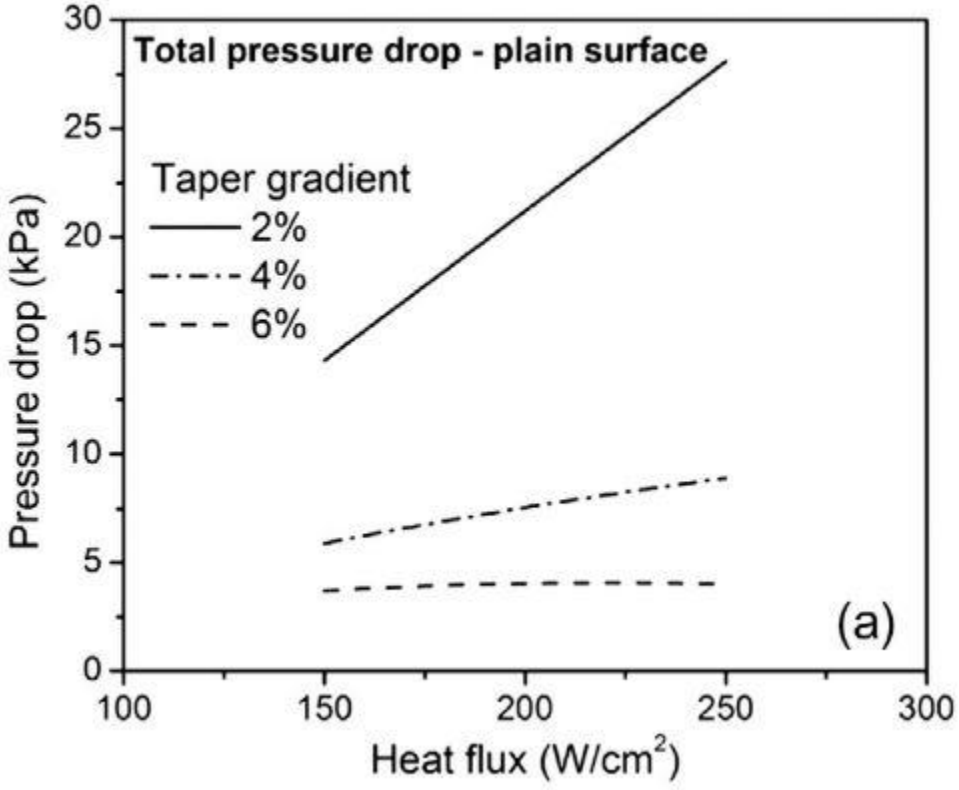

Figure 2. Pressure drop over Plain chip in [6].

Kalani and Kandlikar [4] studied the effect of taper on pressure recovery in open microchannels with a tapered manifold. The flow boiling used water in both plain chips and open microchannels with manifolds with an inlet height of 127 μm before expanding with 2%, 4%, and 6% taper gradients, and modeling pressure drop with a homogeneous flow model, using seven different two-phase viscosity averaging schemes to apply the homogeneous model to the flow. In figure 2,

the total pressure drop decreased in response to increased taper gradient, agreeing with the flow model that the taper angle plays a significant role in maintaining low pressure drops.

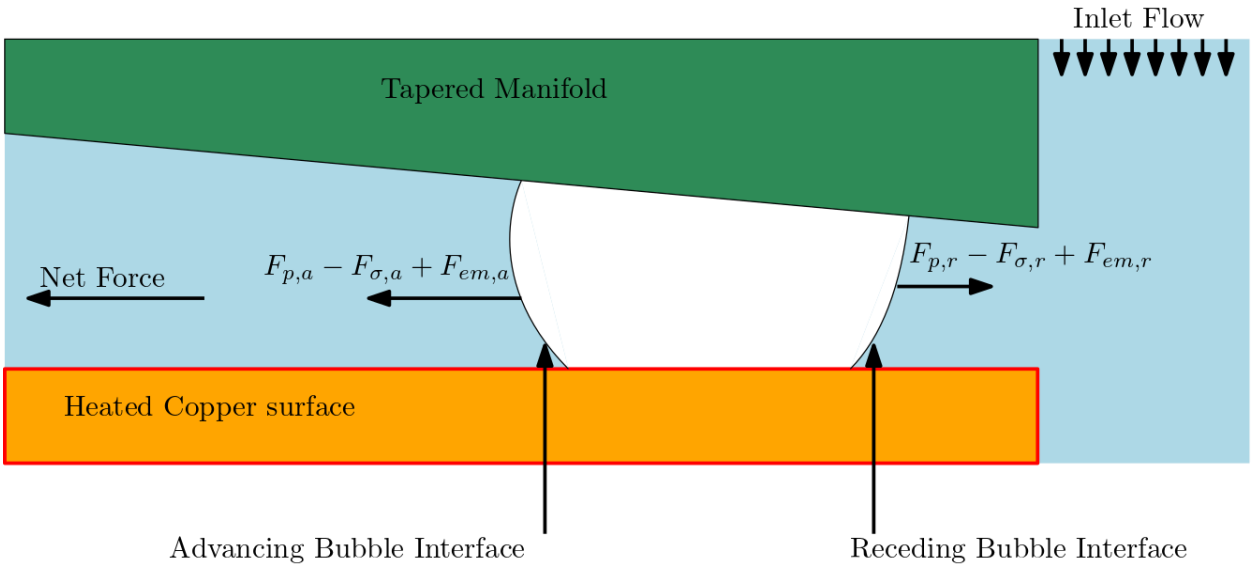

Figure 3. Force Balance for bubble squeezing mechanism, redrawn from [5].

Chauhan and Kandlikar [5] studied using pool boiling with tapered microgaps to create flow boiling sustained entirely by bubble formation in a pool boiling configuration. They studied water boiling in a 10 mm x 10 mm microchanneled copper surface with 10° and 15° taper from inlet microgaps of 1.27 mm. The main takeaway is the introduction of the bubble squeezing mechanism, where the there is a net force in the downstream direction due to the effects of surface tension, pressure, and evaporation momentum forces are more favorable in the downsteam direction, as shown in figure 3. The bubble will expand and move towards the exit, displacing the liquid and drawing liquid in from the inlet region.

2.3 Surface Modification for Pool Boiling Enhancement

Walunj and Sathyabhama [6] Studied the influence of surface roughness on the CHF of water at varied pressure on a 20mm diameter copper surface with unidirectional scratches ranging from

0.106 μm to 4.03 μm. They found that surfaces of higher roughness would become increasingly hydrophilic and increase the bubble departure diameter.

Kwark, et al. [7] performed a parametric study of pressure, orientation, and heater size on the pool boiling performance of water on a heater surface coated with with Aluminum (III) Oxide nanoparticles. They observed that using nanoparticles resulted in an 80% increase in CHF and attributed it to better wetting characteristics thanks to the nanocoating providing a hydrophilic surface. During the downwards-facing orientation, they found that the orientation resulted in high bubble residence time which induced surface dryout much faster than other orientations.

Rainey and You [8] took a double-enhancement approach, investigating combining a “large scale” enhancement technique of vertical fins, with a “small scale” enchancement of a microporous coating on the surface to observe the effects on the boiling of FC-72 over a 10x10mm copper chip. They found significant increases in HTC while CHF appeared to be Insensitive to surface microstructure for the finned surfaces except for the longest fin lengths. They attributed these behaviors as a result of multiple counteracting mechanisms including: surface area enhancement, fin efficiency, surface microstructure, vapor departure resistance, and rewetting liquid flow resistance. It was also observed that surface roughness was significant, with high roughness producing a decrease in wall superheat and an increase in both HTC and CHF.

Chang, et al. [9] Studied boiling heat transfer from longitudinal rectangular finned surfaces immersed in saturated water at low vapor pressures. They varied fin dimensions from 0.5 to 1.0mm, fin height from 0.75 to 15mm and fin thickness from 0.5 to 1.0 and 2.0 mm. Overall, they found that increasing the pressure within the experiment would increase boiling HTC for

both finned and plain surfaces while low pressure boiling formed vapor films and plugs inside the fins at lower fin spacings. At low heat fluxes, it would work

2.4 External Enhancement Methods for Pool Boiling

Mody [10] investigated combining microchannels, volcano manifolds, and dual tapered manifolds with refrigerants PP1, PP1C, and FC-87 in pool boiling on microchannel and plain copper chips. The test section was a 32x34.5 mm copper surface, and the dual tapered manifold had a taper of 15° and an inlet microgap of 0.5 mm. Over the plain chip, the dual tapered manifold increased heat flux by 8.47%, 10.45%, and 5.9% for PP1, PP1C, and FC-87, respectively. From Figure 3, it is shown that the dual tapered manifold extended CHF, but did not significantly enhance HTC. This means that the taper was only really affecting performance at high heat fluxes by supplying more liquid to the surface and keeping nucleate boiling stable. Indicating that it did not really decrease the thermal resistance of the heat transfer process. This behavior was attributed to the small inlet gap of 0.5mm this constricted the inlet significantly. Considering how the major effect was observed at higher heat fluxes, it suggests that the heat flux dependent evaporation momentum force was compensating for the inlet restriction.

Table 1. Pool Boiling performance comparison [2]

Manifold	Plain Chip	Dual-Tapered manifold
Refrigerant	CHF [W/cm^2]	CHF [W/cm^2]
PP1	23.6	25.6
PP1C	28.7	31.7
FC-87	30.5	32.3

Relative to water, Fluorocarbon-based refrigerants have higher density, lower surface tension, so liquid inertia is higher, and the pressure recovery due to the surface tension and pressure forces acting on the expanding bubble interface are less effective, leaving the pumping head to be driven by evaporation momentum and taper area expansion forces.

Chauhan and Kandlikar [11] looked at geometrical effects on heat transfer mechanisms during pool boiling with HFE7000 by testing taper angles between 5 and 25 degrees, and inlet gap heights of 0.8 and 1.27mm. they found up to a 2x enhancement of HTC relative to a plain copper chip.

2.5 Scope of Work

This research focuses on enhancing the pool boiling performance of a copper chip with an exposed boiling surface of 34.5mm x 32mm with PP1C as the working fluid. Few previous works have explored varying the taper angle and inlet gap height for a dual-tapered manifold in pool boiling.

From the literature review, tapered external enhancement structures have been shown to enhance pool boiling performance through pressure recovery effects and bubble squeezing mechanisms with water as the working fluid [5]. However, using the same manifold spacing and taper angle with refrigerants have only demonstrated marginal enhancement as seen in [10].

The novelty of the work stems from varying both the inlet gap height and taper angle of the dual taper angle to observe the effect on passive regulation of the vapor removal and liquid rewetting to the surface.

3. Experimental Setup

3.1 Test Section

The test section for this study is a 34.5 mm x 32 mm rectangular area of copper. This test section is in the center of a circular copper test chip with a 68 mm diameter as shown in Figure 4. Kapton tape is used to mask the surface, covering the test chip and only leaving the test section exposed

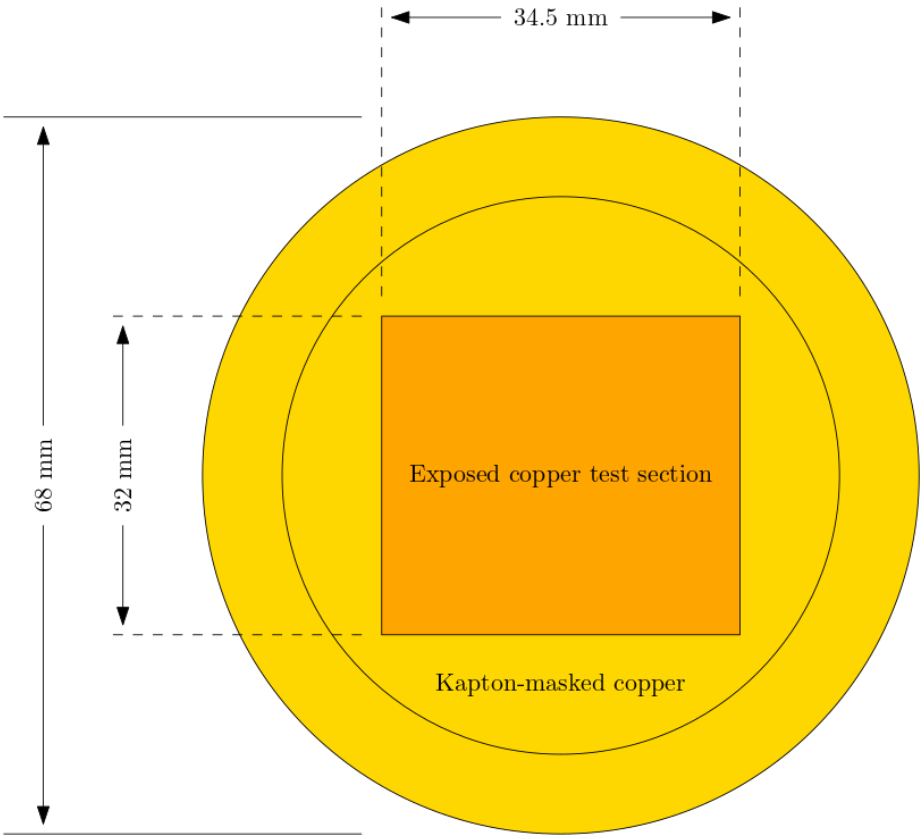

Figure 4. Test section of copper chip.

The top 32 mm x 34.5 mm rectangular surface of a heater block interfaces with the bottom of the test chip to provide thermal energy during experiments. Four electric cartridge heaters each rated for 120V are embedded into the base of the cartridge heater and generate heat through electrical resistance heating. To collect temperature data along the heater block, the ends of three

K-type thermocouples are inserted into three 0.8 mm holes drilled 15 mm into the heater block vertically arranged with 5 mm spacing.

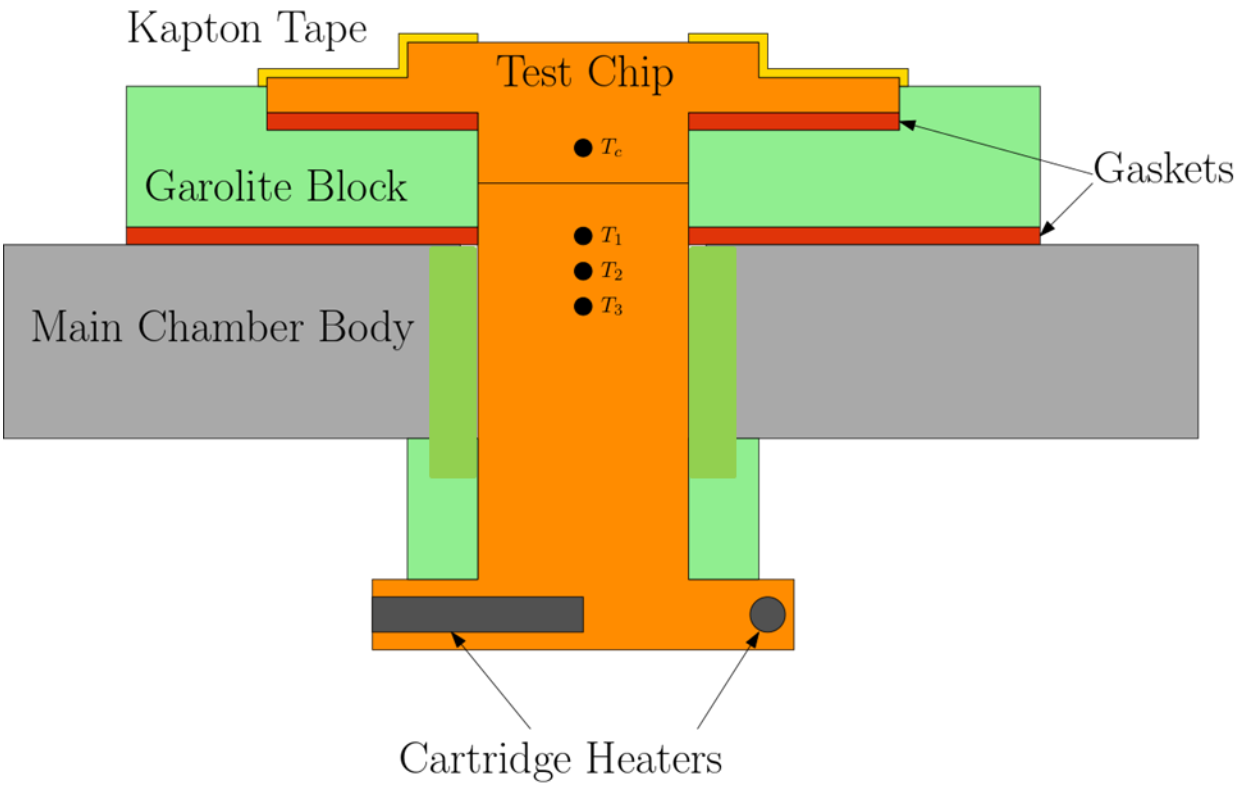

Figure 5. Schematic of test chip and heater block.

The test chip is inserted into a garolite block with a gasket in between the mating surfaces. The assembly is held together by bolts that pass through the holes on the flange geometry of the test chip into corresponding holes with threaded inserts on the recessed surface of the garolite block. First a washer and then a ring gasket are placed onto the bolts so the bolt head will compress the ring gasket to provide a seal. There are two arrangements of holes on the top of the garolite: four corner holes and four threaded auxiliary holes. The auxiliary holes are used to securely mount external enhancement structures. Bolts will be inserted through the corner holes to secure the

garolite block to the test chamber, compressing a rectangular gasket between the mating surfaces of the garolite and test chamber.

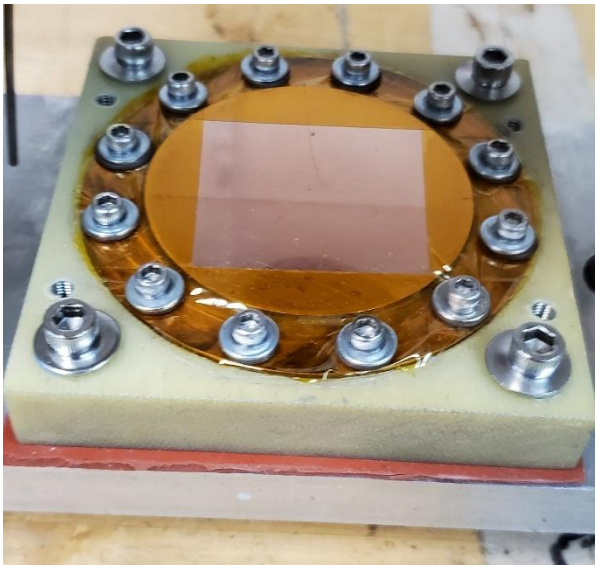

Figure 6. Test Chip and Garolite Block assembly installed in setup.

3.2 Dual Taper Manifold

The Manifolds consists of two components and is shown fully assembled in Figure 7: Side rails and slats. The rails have grooves laser-etched into them of 1 mm width and 1 mm depth while the length is dependent on the desired taper angle. The rails are laser cut from 3 mm thick acrylic

sheet while the slats are laser cut from 1 mm thick acrylic sheet.

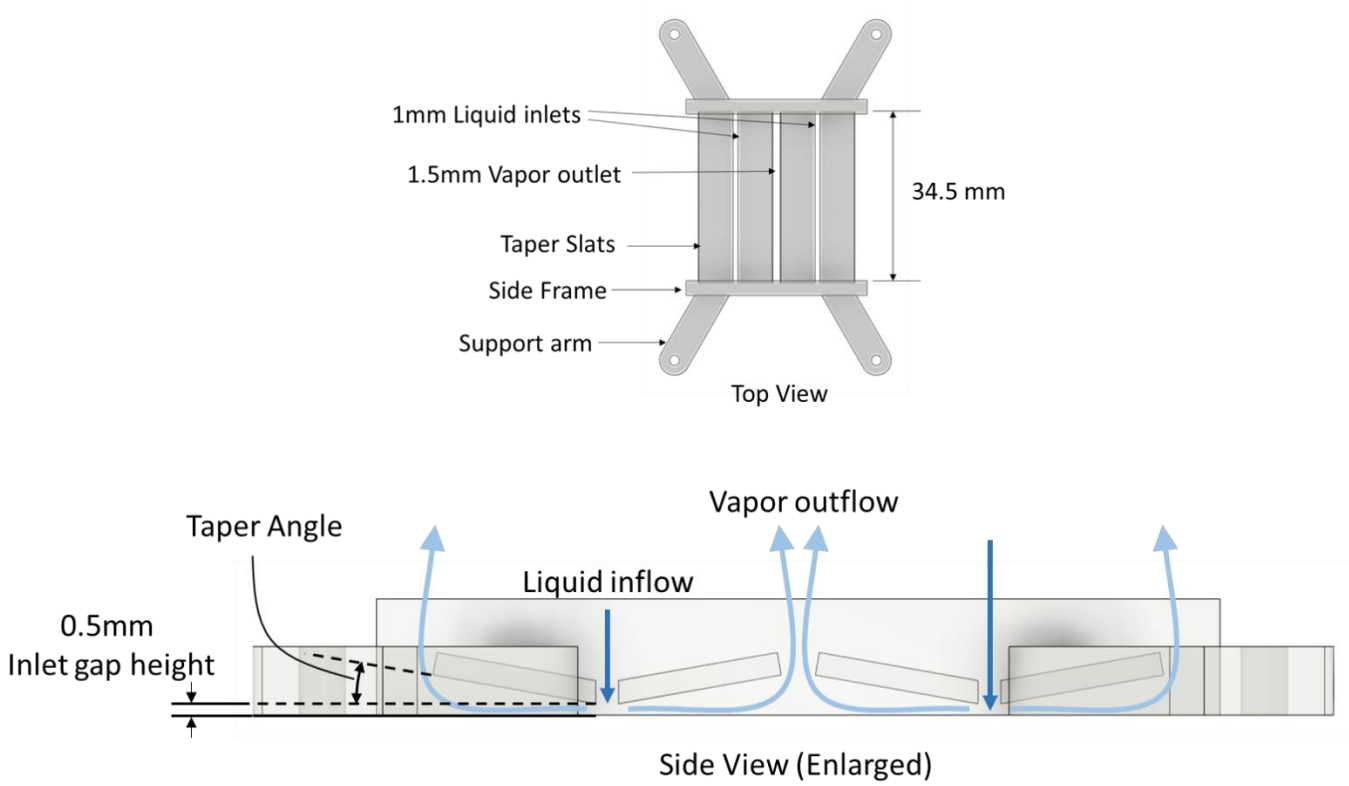

Figure 7. Schematic of process in a manifold

The slats are 36.5 mm long and the width is dependent on the taper angle. The slats are slotted into the grooves on the rails and then acetone is applied near the grooves to join the slats and frame together. A plywood assembly jig was used to assist in assembly and alignment.

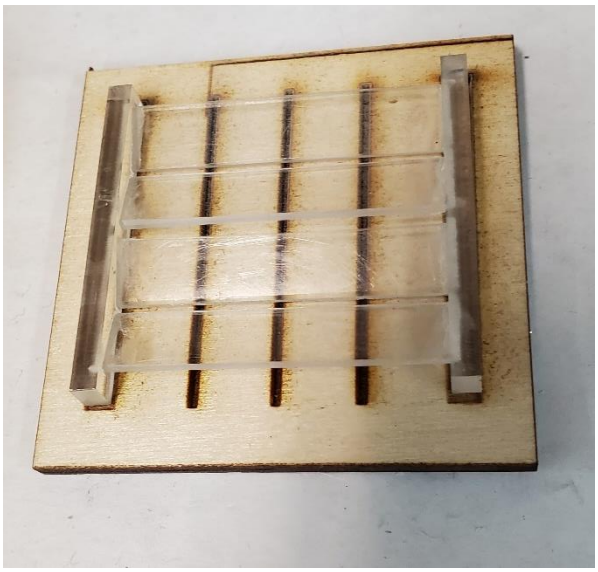

Figure 8. Manifold Parts and Assembly

Two clamps are shown that serve to hold the manifold on top of the test chip.

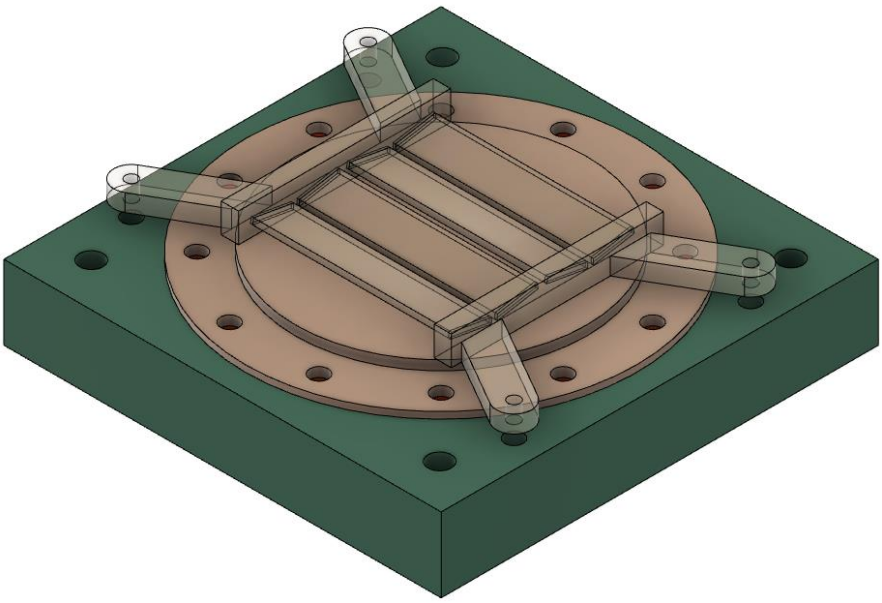

Figure 9 Test Chip and Garolite block assembly with manifold.

Aluminum shim stock is layered beneath the side rails of the manifold to control the vertical spacing.

The Dual taper manifold ideally operates with a self-pumping mechanism. At high heat fluxes, the specific volume increase from liquid changing to vapor provides most of the work for this mechanism. From an initial bubble nucleating and growing until it contacts the taper geometry, the restricted bubble must grow laterally along the surface, and the taper geometry causes growth and bubble motion in the direction of the exit to be more favorable by design. As such, this bubble will grow and move towards the exit and displace liquid, pushing some liquid out of the exit and drawing some liquid in through the inlet. This happens across the entire boiling surface as many bubbles are in various stages of this cycle at any moment.

3.3 Pool Boiling Setup

The pool boiling setup uses an aluminum body with outer dimensions of 6 in x 6 in x 3 in, with a wall thickness of 1 inch. On the top of the body has holes drilled to put the refrigerant in, a pressure gauge, the inlet and outlet of the copper condensing coil, and a hole that connects to a tee-valve that will be used in conjunction with a vacuum pump for degassing the refrigerant. Degassing the perfluorocarbon refrigerant is important due to the ability of gasses to dissolve within the liquid phase.The Pressure gauge is used to read the pressure within the setup. Water is supplied from an external chiller to the condensing coil to maintain atmospheric pressure within the setup and the setpoint temperature is raised/lowered based on the readout from the pressure gauge if the pressure readout is below/above atmospheric, respectively. The thermocouple is used for direct measurement of the saturation temperature of the bulk liquid phase for use in the wall superheat calculation. All holes are ¼” NPT with the exception of the 1/8” NPT thermocouple pass-through. On the bottom of the setup is an auxiliary heater that will be used to heat the bulk liquid to saturation temperature during the initial portion of the experiment. A schematic of the setup is shown in Figure 10.

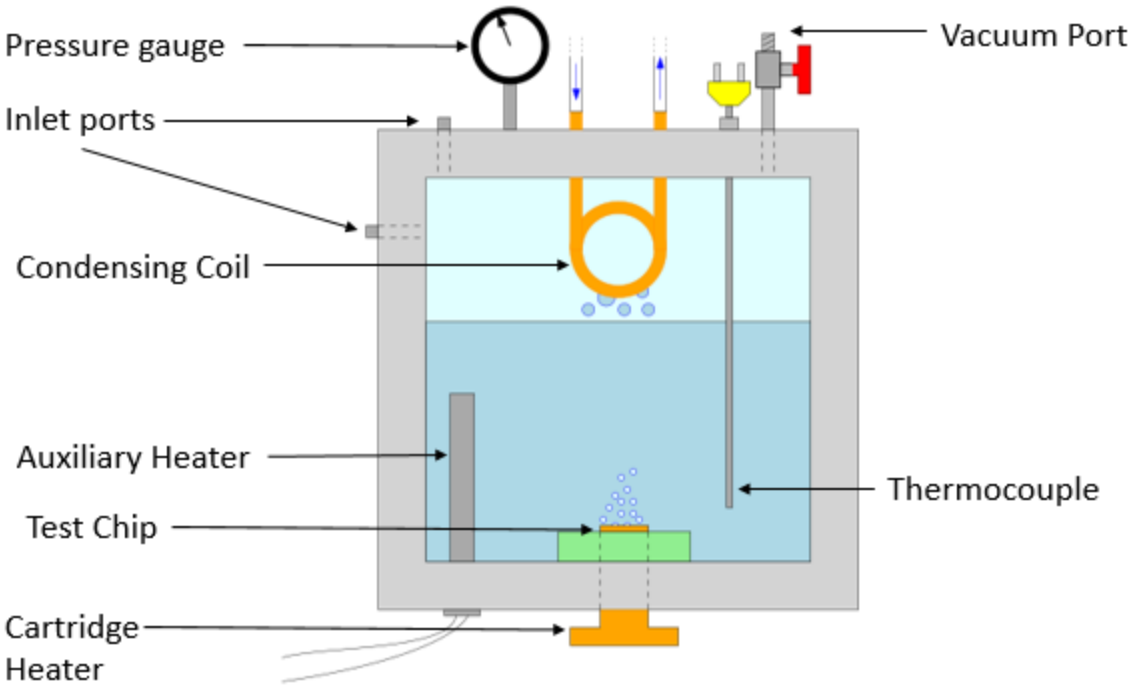

Figure 10. Pool boiling setup schematic.

The front and back of the setup use a combination of two gaskets, borosilicate glass, and aluminum plates to seal and provide a viewing window into the setup.

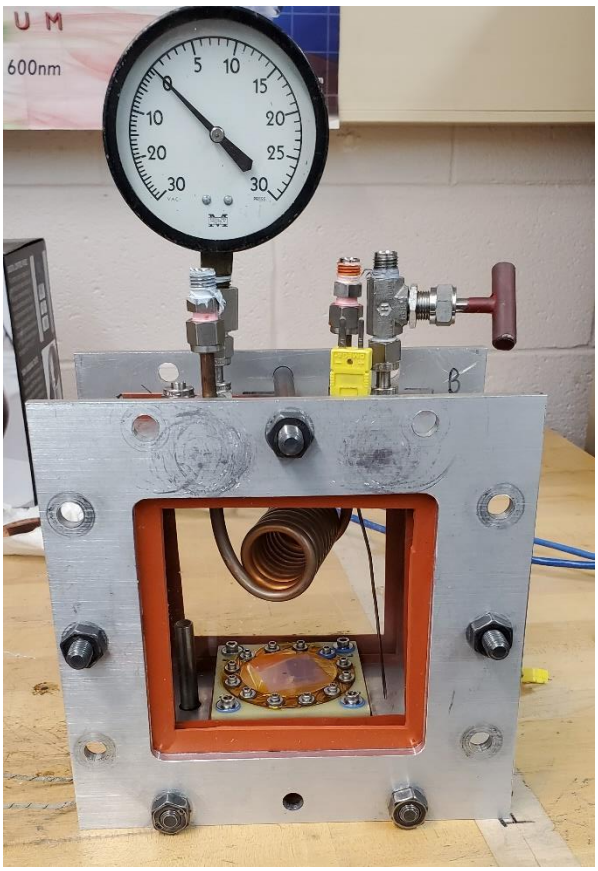

Figure 11. Photo of Pool Boiling setup prior to seal assessment

3.4 Experimental Procedure

- For every experiment, it is important that the test setup is appropriately sealed. Prior to each experiment, the test setup is vacuumed out to -10 psi and let sit for two hours and the pressure loss is evaluated. The experiment proceeded as long as the pressure remained at -10 psi.
- The surface roughness of the test chip is measured prior to each experiment with a laser scanning microscope.
- The test chip is masked with Kapton tape to insulate the non-active heat transfer surfaces.

- The test chip is bolted with twelve 4-40x3/8” socket head bolts into a recessed section of the garolite.
- All bolts within the test chamber use a washer and gasket with the socket head to prevent leaking through the bolt holes.
- Four 8-32x1-3/4” socket head bolts are used to bolt the garolite block to the bottom surface of the aluminum test chamber with a gasket between the garolite and aluminum surfaces.
- 420ml of PP1C is transferred into the test setup with the use of a syringe through an inlet port on top of the chamber.
- The chamber is evacuated to -10 psi (gauge) to remove air within the setup and let stand for 30 minutes to allow the dissolved gasses to leave the refrigerant and re-pressurize the setup.
- The chamber is then re-vacuumed to -10 psi (gauge) to remove most of the residual gasses that have re-pressurized the setup.
- Data acquisition and auxiliary heaters are simultaneously started.
- The LabView program uses a NI-DAQ-9172 and MOD-9211 is used to acquire temperature data from thermocouples.
- The auxiliary heater is supplied an initial voltage of 4V
- The chiller temperature set point is adjusted to maintain atmospheric pressure within the setup.
- Data is recorded for 10 seconds at 5Hz once experiment reaches steady state.
- The power supply voltage is increased by 4V until CHF is reached.

4. Data Acquisition

Equations and methods for finding pool boiling Characteristics:

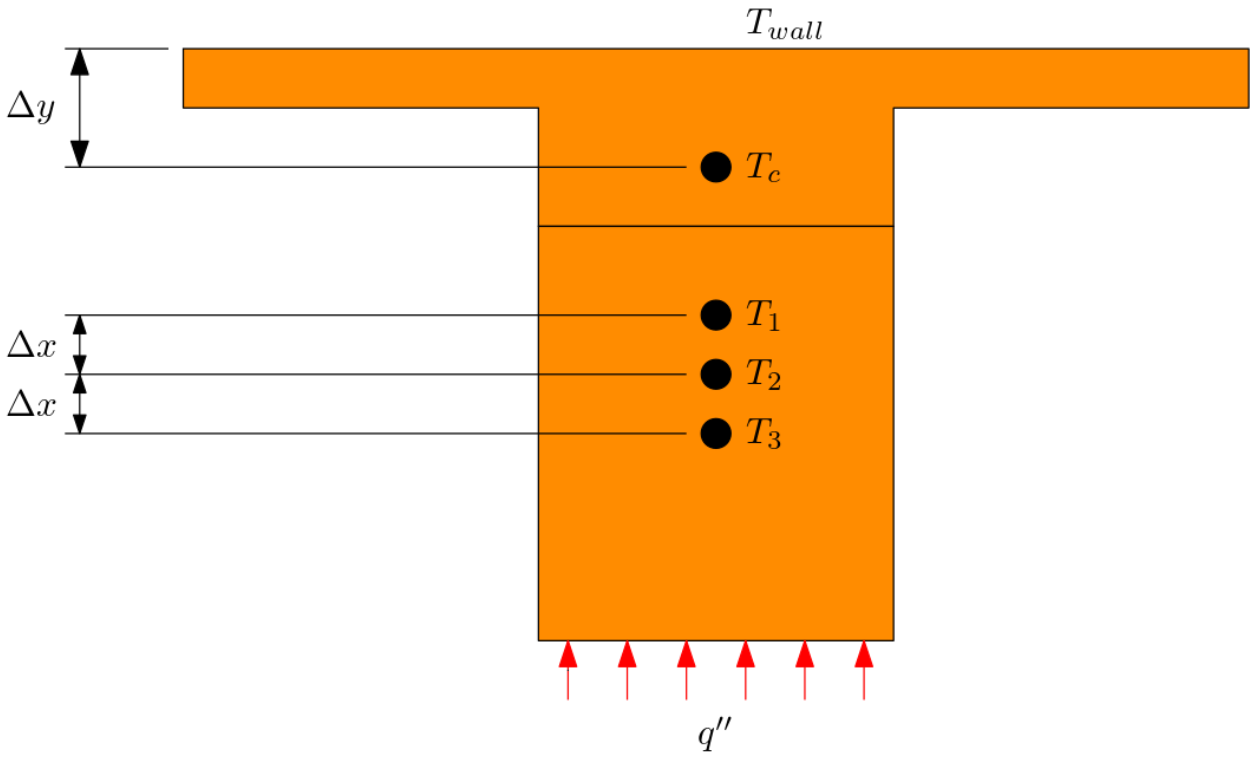

Figure 12. Test chip and heater schematic and thermocouple arrangement

Approximating the first derivative using a backwards finite-difference through three evenly-spaced points has the general form:

$$f'(x_0) \approx \frac{3f(x_0) - 4f(x_0 - h) + f(x_0 - 2h)}{2h} \quad (1)$$

Where f is a function of x, x_0 is the point of interest, and h is the spacing between points

Defining Temperature as the function of interest:

$$\frac{dT}{dx} = \frac{3T_1 - 4T_2 + T_3}{2\Delta x} \quad (2)$$

Where T_1, T_2, and T_3 are the temperatures recorded by the thermocouples in the heater block shown in Figure 8 and Δx is the vertical spacing between the thermocouples.

heat flux can be defined by Fourier's law of 1-D conduction in terms of the temperature gradient and thermal conductivity:

$$q'' = -k\frac{dT}{dx} \quad (3)$$

The wall temperature can be found with the chip temperature, heat flux, vertical spacing from the chip thermocouple to the heater surface, and the thermal conductivity:

$$T_{wall} = T_c - q''\frac{\Delta y}{k} \quad (4)$$

The heat transfer coefficient between the surface and working fluid can be found in terms of the heat flux, wall temperature, and saturation temperature.

$$HTC = \frac{q''}{T_{wall} - T_{sat}} \quad (5)$$

5. Uncertainty Analysis

The uncertainty analysis in this study is similar to that in Mody's work. Uncertainty in thermocouple calibration, inter-thermocouple distances, material thermal conductivity all contribute to the overall uncertainty in data analysis calculations. Uncertainty can be separated into two types: Bias and Precision errors.

$$U_p = \sqrt{{B_y}^2 + {P_y}^2} \tag{6}$$

Precision errors come from errors in the calibration process, and is found by taking the standard deviation at each calibration temperature, then taking the overall average of standard deviatons, and then doubling it to obtain a 95% confidence interval. Bias errors arise in the experimental data, where it is the standard deviation of values from the mean value in a particular set of steady-state data.

errors will propagate through data analysis calculations, including temperature gradient, heat flux, surface temperature, wall superheat, and HTC.

The uncertainty of a calculated parameter depends on the uncertainty of the parameters it is calculated from. A commonly used formula is as follows:

$$U_A = \sqrt{\sum_1^n \left(\frac{\partial A}{\partial a_i} u_{a_i}\right)^2} \tag{7}$$

Where U_A is the uncertainty in the calculated parameter A, and u_{a_i} is the uncertainty of an independent parameter a_i. Applying this to the heat flux equation and factoring out heat flux from the right hand side terms:

$$U_{q''} = q'' \sqrt{\left(\frac{u_{k_{cu}}}{k_{cu}}\right)^2 + \left(\frac{u_{\Delta x}}{\Delta x}\right)^2 + \frac{\left(u_{T_1}\right)^2 + \left(u_{T_2}\right)^2 + \left(u_{T_3}\right)^2}{(3T_1 + 4T_2 + T_3)^2}} \quad (8)$$

Fourier's law of 1-D conduction is used in finding the heat flux through the heater block, And the temperature gradient is more extreme at higher heat fluxes but still remains linear. The high r^2 value of the linear fits confirm that these temperature profiles are effectively linear for the heat fluxes observed in these experiments with negligible losses.

Applying this to the HTC calculation

$$U_{HTC} = HTC \sqrt{\left(\frac{u_{w_{sup}}}{w_{sup}}\right)^2 + \left(\frac{U_{q''}}{q''}\right)^2} \quad (9)$$

6. Results and Discussions

The primary objective of this study is to analyze the effect of changing dual-tapered manifold design parameters on boiling heat transfer performance by passively affecting the flow of liquid and vapor over a boiling surface. PP1C was used with a plain copper chip. Tests were performed under increasing heat flux through external power and increasing it at regular intervals. Data was recorded when the system reached steady state. Heat flux was regularly increased up until CHF is reached and then subsequently stopped.

6.1 Plain Chip

A baseline was obtained with a plain copper chip of area 34.5 x 32mm for heat transfer at atmospheric conditions. The results are shown in Figure 11. A CHF of 21.5 W/cm^2 was obtained at a wall superheat of 19.6°C for PP1C. The peak HTC was found at 14.4 kW/m^2 K at a heat flux of 17.9 W/cm^2 at a wall superheat of 12.5°C.

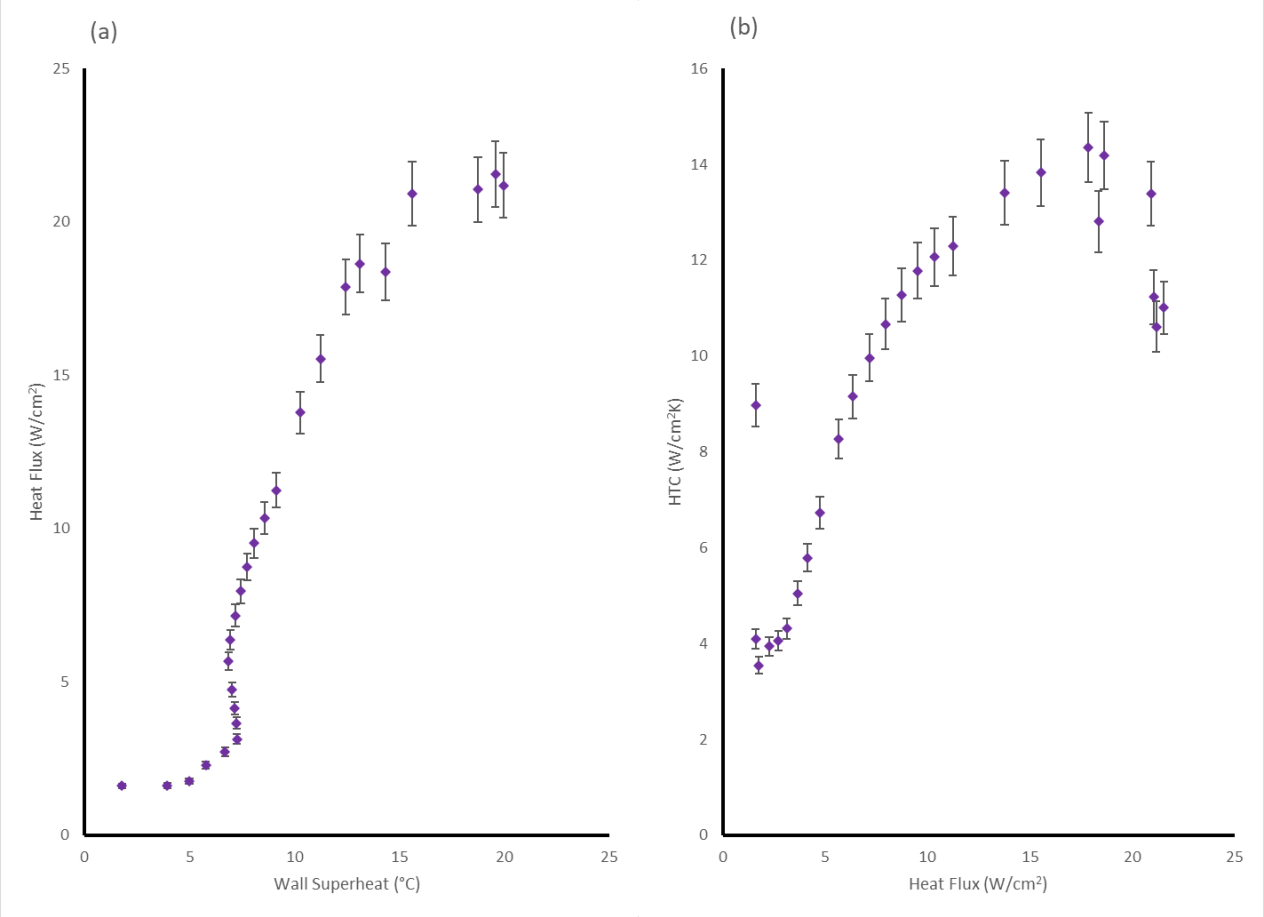

Figure 13. (a) Pool Boiling curve and (b) HTC for PP1C with plain copper chip.

6.2 Dual Taper Manifolds at 0.5mm spacing

At 0.5mm spacing, a CHF of 14.6, 16.6, and 19.3 W/cm^2 was obtained at a wall superheat of 23.2, 24.7, and 26.1°C for 10, 15, and 20 degree taper angle, respectively. The results are shown in Figure 12.

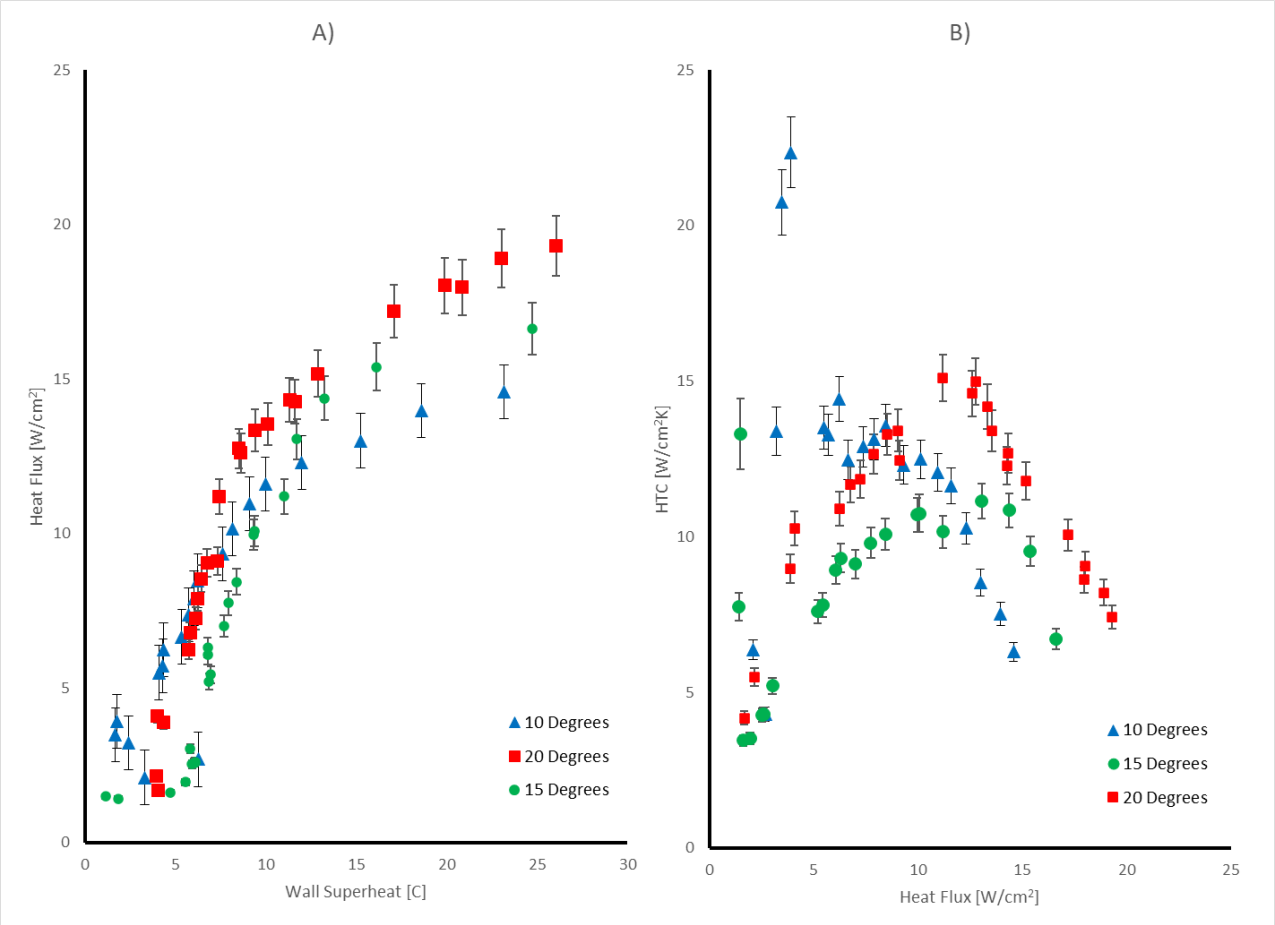

Figure 14. (a) Boiling curve and (b) HTC for manifolds at 0.5 mm inlet gap height.

Additionally: A peak HTC of 14.1, 11.1, and 15.1 kW/m^2°C were found for 10, 15, and 20 degrees, respectively. Relative to the plain chip CHF, the 10 degree manifold demonstrates the lowest CHF, while the 15 and 20 degree manifolds are progressively better, but still poorer than the plain chip performance. Peak HTC performance was worse than baseline for 10 degree taper angle, with the 15 degrees being even worse. Conversely, the 20 degree manifold demonstrated marginal improvement in peak HTC. The taper geometry appeared to interact with the bubbles which appeared to be squeezed, but this only seemed to increase the residence time of the bubbles and not promote fluid circulation.

6.3 Dual Taper Manifolds at 1mm spacing

At 1.0 mm spacing, a CHF of 18.9, 22.7, and 23.3 W/cm^2 was obtained at a wall superheat of 17.9, 18.1, and 24.4 °C for 10, 15, and 20 degree taper angle, respectively. The results are shown in Figure 13.

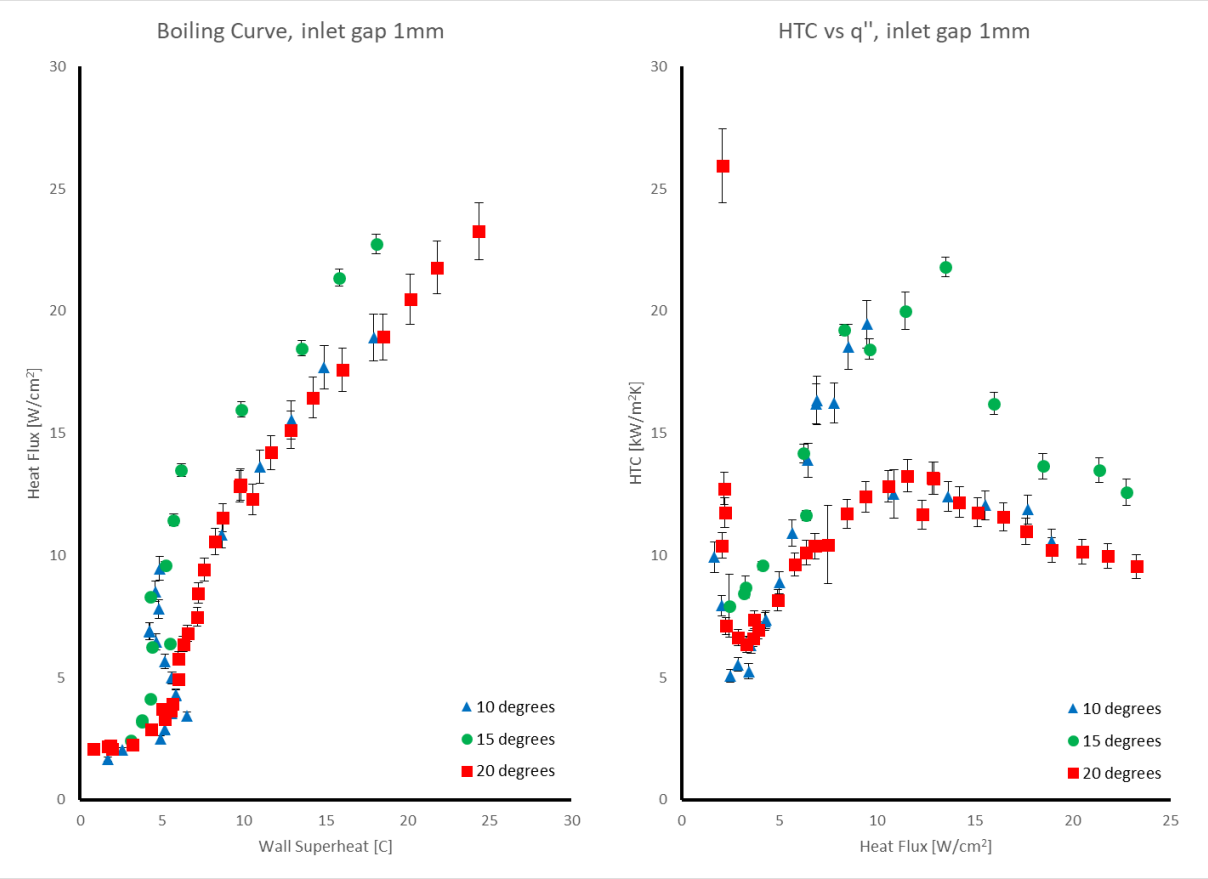

Figure 15. (a) Boiling Curve and (b) HTC curve for manifolds at 1mm inlet gap height.

Additionally: A peak HTC of 19.5, 21.8, and 13.3 kW/m^2 °C were found for 10, 15, and 20 degrees, respectively. CHF was worse than baseline for the 10 degree manifold, while the 15 degree manifold showed slight improvement, and the 20 degree followed this trend with even better CHF. In terms of peak HTC, the 10 and 15 degree manifolds show significant HTC enhancement while the 20 degree manifold worsened peak HTC. the HTC of the 10 and 15

degree manifolds increase rapidly with respect to heat flux before hitting the peak and then severely dropping off. The notable effect of these

6.4 Dual Taper Manifolds at 1.5mm Spacing

At 1.5mm spacing, a CHF of 19.2, 21.6, and 20.8 was obtained at a wall superheat of 19.0, 18.8, and 17.3°C for 10, 15, and 20 degree taper angle, respectively The results are shown in Figure 14. Additionally: A peak HTC of 14.6, 15.9, and 15.1 kW/m^2 °C were found for 10, 15, and 20 degrees, respectively.

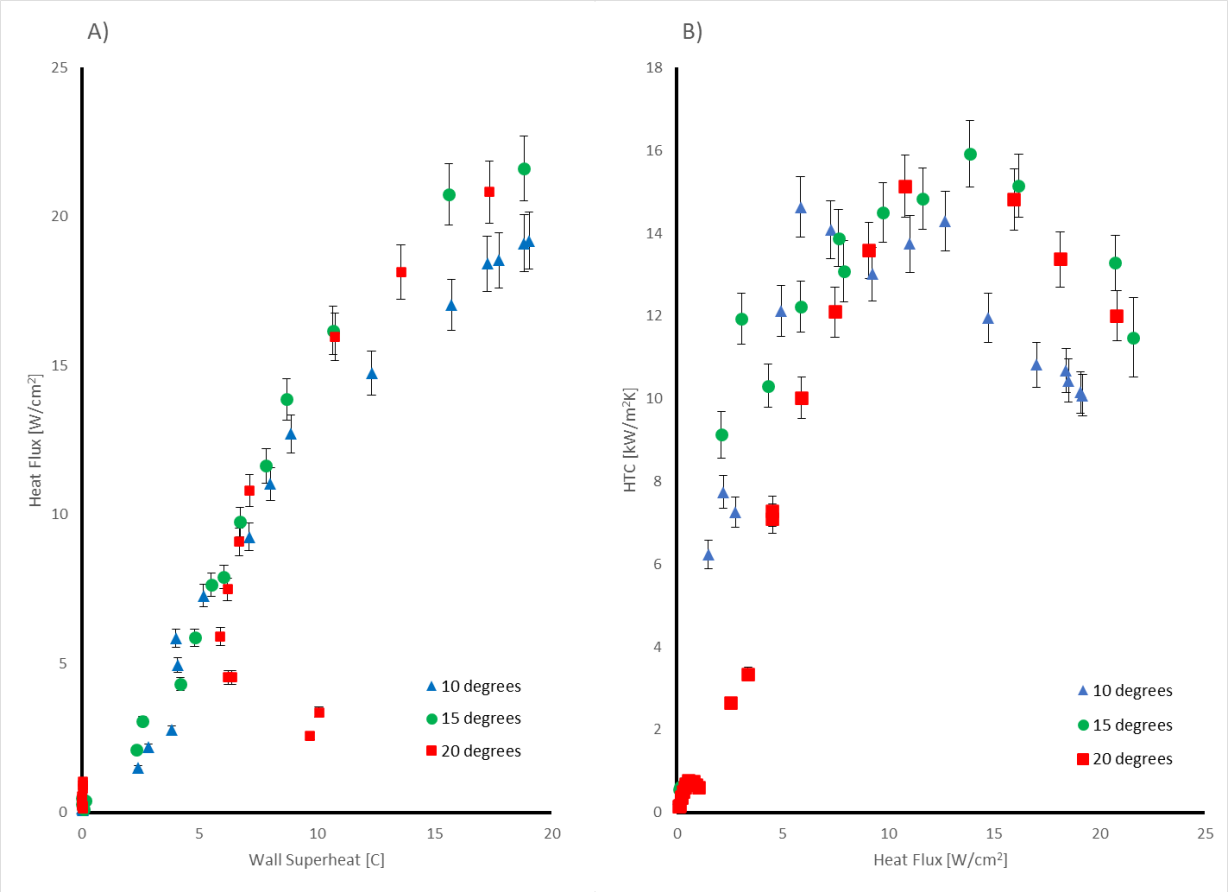

Figure 16. Plot of (a) Boiling and (b) HTC curves for manifolds at 1.5mm inlet gap height

Relative to the plain chip, the 10 degree manifold performed worse in terms of both CHF and peak HTC, while the 15 degree manifold showed marginal improvement and the 20 degree manifold was only slightly worse.

6.5 Performance Characteristics vs Inlet gap height

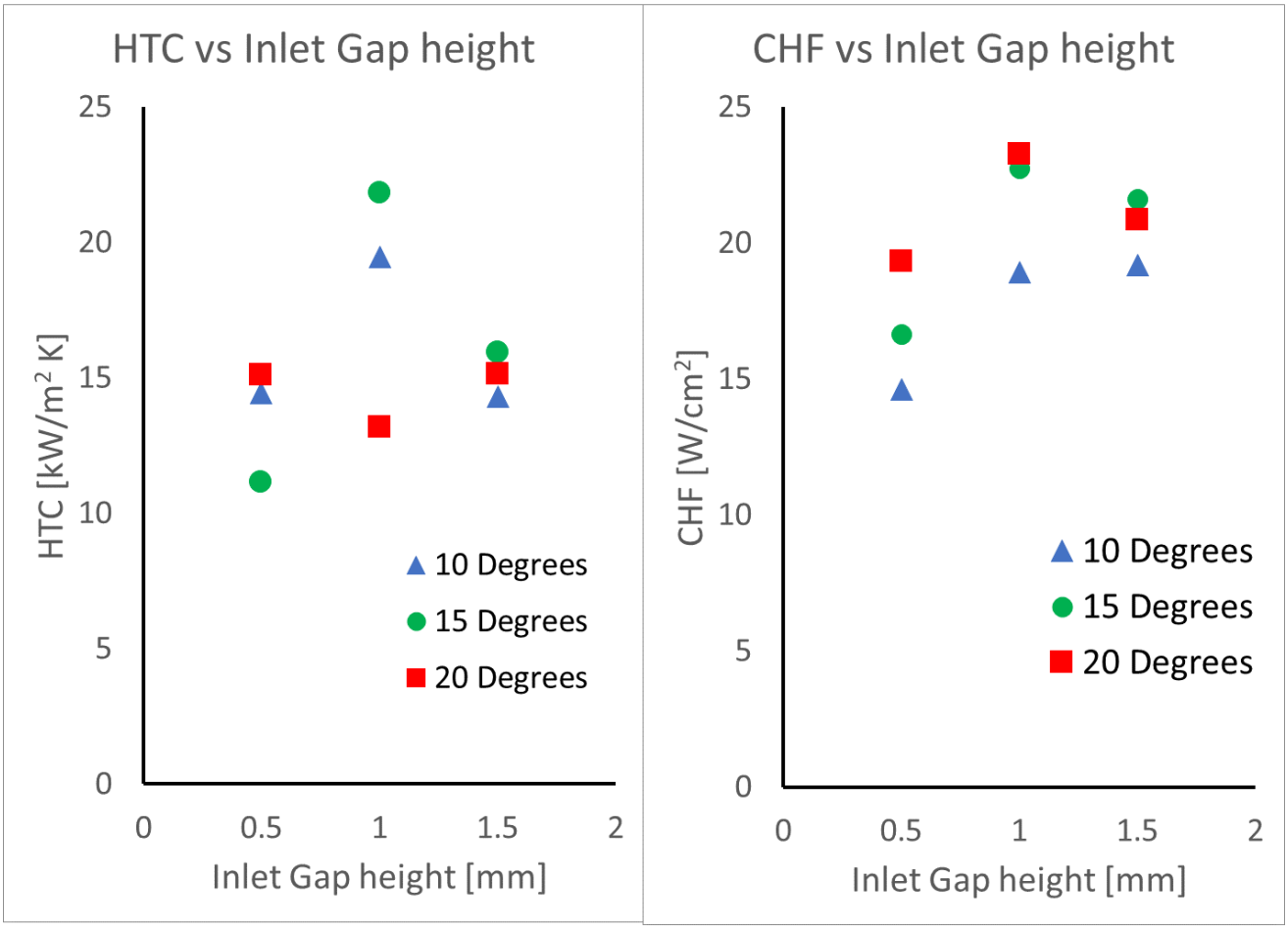

Figure 17. Pool boiling characteristics vs Inlet gap height

Here, the behavior of the performance characteristics is interesting. For the higher taper angles, the CHF starts off subpar at 0.5mm inlet gap height, and then peaks at 1mm for both the 15 and 20 degree manifolds, and increasing it to 1.5mm reduces the benefit. For the 10 degree manifold,

the CHF notably increases from 0.5 to 1mm and then marginally increases when increasing the inlet gap to 1.5mm.

6.6 Performance Characteristics vs Exit gap height

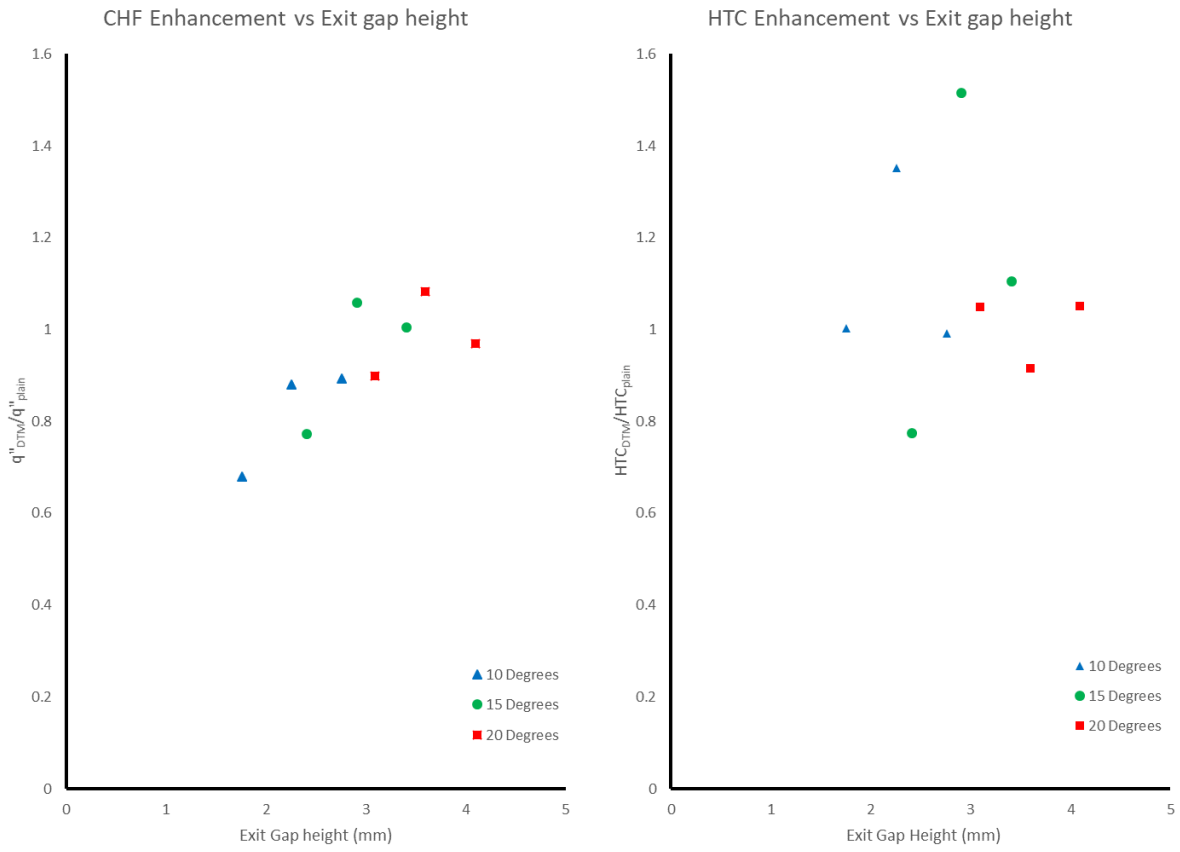

Figure 18 Enhancement Factors of Dual Taper manifold vs Exit gap height

Comparing the factor of enhancement for HTC and CHF to the exit gap height is interesting. CHF demonstrates a positive correlation with the exit gap height. A positive trend is observed, but the present data set suggests there is an upper limit to this enhancement that is insignificant when compared to other enhancement techniques.

The HTC enhancement appears to have a weakly positive correlation with exit gap height, appearing very scattered. indicating that. Looking at the CHF, a much stronger positive correlation is observed, although the enhancement factor is initially at around 0.7 at the lowest and the maximum observed is 1.1. Overall, the CHF does not seem to be enhanced by the present manifolds, as the specific volume of PP1C does not significantly increase during the phase change from liquid to vapor. This prevents evaporation momentum force from effectively pumping the flow at higher heat fluxes and does not really serve to extend CHF. Notably, all of the exit gap heights exceed the bubble departure diameter for PP1C, so there a point under the manifold where growing bubbles detach from the surface and that significant portions of the heater surface are not squeezing bubbles and regular pool boiling is exhibited.

7. Conclusions

The present study, PP1C was tested for its pool boiling performance at atmospheric pressure on a test section of 32 mm x 34.5 mm in a closed pool boiling setup. This study focuses on varying the inlet gap height and taper angle of the dual-taper manifold to observe the effect on pool boiling performance. The setup explores three different manifold taper angles at three inlet gap heights for a total of nine configurations. Overall, the current system does not enhance in boiling significantly in respect to performance characteristics.

- High specific volume increase in the transition from liquid to vapor is very important for bubble squeezing mechanism to be effective. The specific volume of PP1C doesn't increase as much when compared to water, making it an undesirable fluid for the bubble squeezing mechanism.
- High thermal conductivity of the liquid phase is likewise very important for faster vaporization of the liquid into vapor and provide higher velocity for evaporation momentum force.
- For a plain copper chip, a CHF of 21.5 W/cm^2 was achieved at a wall superheat of 19.5
- Increasing the inlet gap height did not show any overall trend in enhancing pool boiling performance- 0.5mm inlet gap saw a decrease in CHF, 1mm inlet gap showed minor enhancement for 15 degree and 20 degree manifolds. Increasing the inlet gap to 1.5mm did not show much effect relative to 1mm.
- For all manifolds at 0.5mm, CHF was lower than Plain chip. The 10 degree manifold demonstrated the poorest CHF, while the 15 and 20 degree manifold performed progressively better but still worse than the plain chip.

- For the set of manifolds at 1mm, the 10 degree manifold performed worse than the plain chip, while the 15 and 20 degree manifold performed better as taper angle increased.
- At 1.5mm, the 15 degree manifold demonstrated the best CHF, although marginally better than the plain chip, while the 10 and 20 degree manifolds decreased CHF.
- For the 20 degree taper angle, HTC was improved at 0.5mm and 1.5mm and was negatively impacted at 1mm. Conversely, CHF was improved at 1mm spacing, and negatively impacted at 0.5mm and 1.5mm spacings.
- Varying the taper angle showed an effect on pool boiling performance: for each inlet gap variation, CHF increased relative to increasing the taper angle.
- Both the inlet gap height and taper angle are both important for interacting with growing bubbles for adequate squeezing. A large inlet gap and an aggressive taper will only squeeze growing bubbles near the inlet and the bubbles will detach from the heater surface prior to leaving the manifold due to growing too large.

8. Recommendations for future work

- This study evaluated the effect of taper angle and inlet gap height of a dual-tapered manifold on the boiling performance of PP1C over a copper surface experimentally.
- Overall, the Dual-taper manifold performs very poorly with PP1C because of the liquid-vapor density increase being relatively small when compared to that of water- which the dual-tapered manifold works well with. As such, it is recommended to not pursue this enhancement technique with fluids that have small liquid vapor-density ratios.
- The manifold design in this study serves to squeeze expanding bubbles, but they appear to freely expand perpendicular to the expanding taper direction. To remedy this, future design iterations could incorporate flow partitions to force the bubbles to expand along the flow direction.
- Since the local height of the tapered geometry is important for effective squeezing, future studies could investigate the modifying the length of the individual tapered sections when used for a larger heat transfer surface and increasing the number of dual-taper sections present in order to match the footprint of the boiling surface to increase the area on the surface where bubble squeezing can occur.

9. References

[1] Rainey, K. N., and You, S. M., 2001, "Effects of Heater Size and Orientation on Pool Boiling Heat Transfer from Microporous Coated Surfaces," Int. J. Heat Mass Transf., **44**(14), pp. 2589–2599.

[2] Mukherjee, A., and Kandlikar, S. G., 2009, "The Effect of Inlet Constriction on Bubble Growth during Flow Boiling in Microchannels," Int. J. Heat Mass Transf., **52**(21–22), pp. 5204–5212.

[3] Kalani, A., and Kandlikar, S. G., 2015, "Combining Liquid Inertia with Pressure Recovery from Bubble Expansion for Enhanced Flow Boiling," *Appl. Phys. Lett.*, **107**(18), p. 181601.

[4] Kalani, A., and Kandlikar, S. G., 2015, "Effect of Taper on Pressure Recovery during Flow Boiling in Open Microchannels with Manifold Using Homogeneous Flow Model," Int. J. Heat Mass Transf., **83**, pp. 109–117.

[5] Chauhan, A., and Kandlikar, S. G., 2020, "Transforming Pool Boiling into Self-Sustained Flow Boiling through Bubble Squeezing Mechanism in Tapered Microgaps," Appl. Phys. Lett., **116**(8), p. 081601.

[6] Walunj, A., and Sathyabhama, A., 2019, "Bubble Dynamics and Enhanced Heat Transfer during High-Pressure Pool Boiling on Rough Surface," J. Thermophys. Heat Transf., **33**(2), pp. 309–321.

[7] Kwark, S. M., Amaya, M., Kumar, R., Moreno, G., and You, S. M., 2010, "Effects of Pressure, Orientation, and Heater Size on Pool Boiling of Water with Nanocoated Heaters," Int. J. Heat Mass Transf., **53**(23–24), pp. 5199–5208.

[8] Rainey, K. N., and You, S. M., 1999, “POOL BOILING HEAT TRANSFER FROM PLAIN AND MICROPOROUS, SQUARE PIN FINNED SURFACES IN SATURATED FC-72,” ASME International Mechanical Engineering Congress and Exposition, Proceedings (IMECE), pp. 245–253.

[9] Chang, J. Y., and You, S. M., 1997, “Boiling Heat Transfer Phenomena from Micro-Porous and Porous Surfaces in Saturated FC-72,” Int. J. Heat Mass Transf., **40**(18), pp. 4437–4447.

[10] Mody, F., Evaluation of External Surface Modification Techniques to Evaluation of External Surface Modification Techniques to Enhance Pool Boiling of Dielectric Fluids Enhance Pool Boiling of Dielectric Fluids.

[11] Mody, F., Chauhan, A., Shukla, M., & Kandlikar, S. G. (2022). Evaluation of heater size and external enhancement techniques in pool boiling heat transfer with dielectric fluids. *International Journal of Heat and Mass Transfer, 183*.